JGR Oceans

RESEARCH ARTICLE
10.1029/2022JC018756

Key Points:

- Virtual Lagrangian particles were launched in the Labrador Current upstream of the Tail of the Grand Banks, using an eddy-resolving model
- The presence of Gulf Stream eddies at the Tail of the Grand Banks strongly modulates westward transport in the Labrador Current
- Interannual variability in the impingement of Gulf Stream eddies has prevented westward penetration of the Labrador Current in recent years

Correspondence to:
A. Gonçalves Neto,
afonso@uri.edu

Citation:
Gonçalves Neto, A., Palter, J. B., Xu, X., & Fratantoni, P. (2023). Temporal variability of the Labrador Current pathways around the tail of the Grand Banks at intermediate depths in a high-resolution ocean circulation model. *Journal of Geophysical Research: Oceans*, *128*, e2022JC018756. https://doi.org/10.1029/2022JC018756

Received 13 APR 2022
Accepted 18 FEB 2023

Temporal Variability of the Labrador Current Pathways Around the Tail of the Grand Banks at Intermediate Depths in a High-Resolution Ocean Circulation Model

Afonso Gonçalves Neto[1,2], Jaime B. Palter[1], Xiaobiao Xu[3], and Paula Fratantoni[4]

[1]Graduate School of Oceanography, University of Rhode Island, Narragansett, RI, USA, [2]Department of Oceanography, Federal University of Santa Catarina, Florianópolis, Brazil, [3]Center for Ocean-Atmospheric Prediction Studies, Florida State University, Tallahassee, FL, USA, [4]NOAA NMFS Northeast Fisheries Science Center, Woods Hole, MA, USA

Abstract The Northwest Atlantic Shelf and Slope have warmed dramatically in the past decade, changing marine life and challenging fisheries management. A rapid warming event in 2009/2010, linked to a reduced supply of cold water from the Labrador Sea, pushed this region to a new state of unprecedentedly high temperatures that persists today. However, a mechanistic understanding of how the Labrador Current connectivity is reduced at the Tail of the Grand Banks of Newfoundland has been lacking. Here, we present the results of a 25-year (1993–2017) Lagrangian analysis using the HYbrid Coordinate Ocean Model. Synthetic particles were released in the vicinity of the Labrador Current upstream of the Grand Banks and tracked in a 2-D velocity field. We found that the Labrador Current can be completely blocked by Gulf Stream eddies and meanders that impinge on the shelf break along the Grand Banks. This blocking can occur in many different locations at, upstream, or downstream of the Tail of the Grand Banks, since the Labrador Current needs a clear passage over a long distance to continue its path. In the simulation, the Labrador Current has been blocked more often since 2008, which led to the warming of the Northwest Atlantic Shelf and Slope. These results, which are consistent with satellite observations, can provide predictability for the New England and Nova Scotia shelf environments potentially helpful for ecosystem management.

Plain Language Summary The New England and Nova Scotia continental shelves have been warming at a rate much faster than almost anywhere else in the global ocean. Just east of this region, two of the Atlantic's mightiest currents—the warm Gulf Stream and the cold Labrador Current—interact near the edge of an underwater plateau called the Grand Banks of Newfoundland. Previous observational work suggested that the warming of the continental shelf has been caused by the rising proportion of Gulf Stream waters, due to the reduced contribution of Labrador Current as it rounds the Grand Banks. Here, we use an ocean model that simulates circulation in this region with excellent accuracy to take a deeper look at the drivers of this blockage of the Labrador Current. The model suggests that when the swirling Gulf Stream eddies approach the Grand Banks, they prevent the Labrador Current from continuing its journey to the west, ultimately starving the New England and Nova Scotia continental shelves of a source of cold, fresh water. Because the Gulf Stream eddies have a clear sea surface height signature, an indication of these blocking dynamics may be observed by satellite.

1. Introduction

The Northwest Atlantic Shelf is one of the fastest warming regions in the ocean (Bulgin et al., 2020). The accelerated warming experienced since 2008 has contributed to the conditions for large marine heat waves, challenged fisheries management (Mills et al., 2013; Pershing et al., 2018), and has been blamed for the northward migration and increasing entanglement of North Atlantic Right Whales (Meyer-Gutbrod et al., 2021). Studies using ocean circulation models have linked water mass shifts on the Scotian Shelf and in the Gulf of St. Lawrence to changes in the westward transport of the Labrador Current (Brickman et al., 2018; Claret et al., 2018). Claret et al. (2018) further showed that a decrease in the connectivity of the Labrador Current past the shallow underwater plateau known as the Grand Banks of Newfoundland is predicted to intensify the deoxygenation of the Gulf of St. Lawrence under the global warming associated with a hypothetical doubling of atmospheric CO_2. Specifically, their model simulation associated warming with circulation changes originating at the southeastern tip of the Grand Banks.

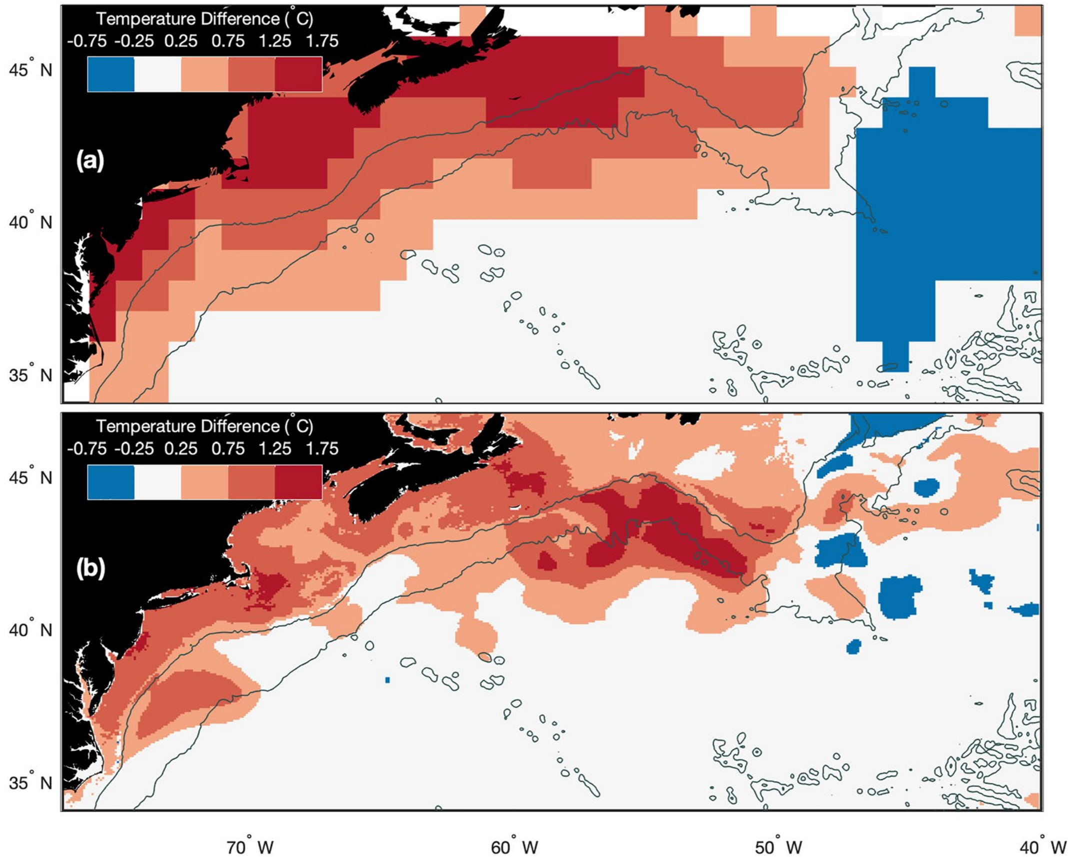

Figure 1. Observed and modeled temperature change in the Northwest Atlantic. (a) Vertically averaged ocean temperature change from the EN4 objective analysis to 2,000 m, or the seafloor if it is shallower than 2,000 m, for the period 2009–2018 minus 2001–2008. (b) Vertically averaged ocean temperature change from Hybrid Coordinate Ocean Model between the model layers 1 and 20 for the period 2009–2018 minus 2001–2008. In both panels, the color contours show 0.5°C increments (change in the unshaded region is between −0.25 and 0.25°C), and the 1,000 and 4,000-m isobaths are shown in dark gray contours.

In this region, commonly referred to as the Tail of the Grand Banks (Figure 1), a ridge extends southeastward from the main plateau with an ocean depth of 3–4 km. Here, the Gulf Stream interacts with both the complex bathymetry and the Labrador Current. Analysis of the long-term observational data indicates that in the region between Flemish Cap and the Tail of the Grand Banks, the Labrador Current waters can be ejected from the boundary and transported eastward into the subpolar North Atlantic interior, but little is known about the mechanisms controlling these circulation pathways nor how they might vary from year to year (Fratantoni & McCartney, 2009; Fratantoni & Pickart, 2007). An analysis of 26 years of satellite altimetry revealed that positive sea surface height anomalies at the Tail of the Grand Banks are associated with a slowing of the Labrador Current all along the Scotian and Northeast US Slope (Gonçalves Neto et al., 2021). The slowing of the Labrador Current is accompanied by progressive warming of the shelf waters. An abrupt increase in sea surface height at the Tail of the Grand Banks in 2008 preceded the rapid subsurface warming that propagated from the Gulf of St. Lawrence to the Gulf of Maine in 2009 and 2010. Therefore, monitoring sea surface height at the Tail of the Grand Banks may provide predictability for environmental conditions on the shelf. It remains unknown, however, how the sea surface height increase results in reduced westward connectivity of the Labrador Current.

The complex circulation and bathymetry at the Tail of the Grand Banks, combined with a lack of substantial long-term water column observations, challenges our understanding of the mechanisms that are associated with the shift in sea surface height and disruption of Labrador Current continuity. Lagrangian analyses have been used to explore circulation features near the Tail of the Grand Banks: The discovery that Lagrangian floats within the Labrador Sea Water layer were ejected from the boundary at Flemish Cap and the Tail of the Grand Banks (Bower et al., 2009, 2011) disrupted the long-standing hypothesis of continuity of the Deep Western

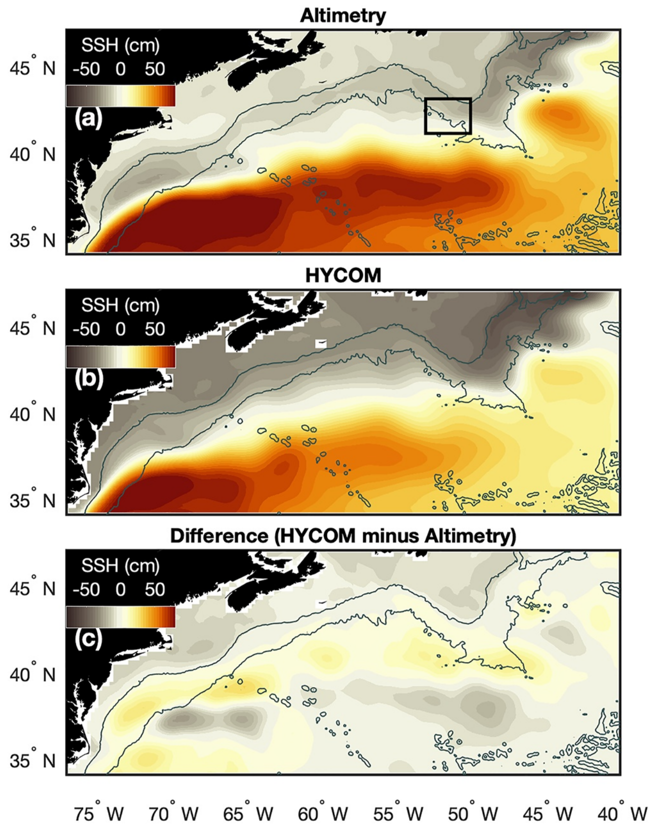

Figure 2. Mean sea surface height in the Northwest Atlantic Ocean for the period 1993–2017 (a) from altimetry and (b) in the Atlantic Hybrid Coordinate Ocean Model (HYCOM) output. (c) The spatial difference in sea surface height between the HYCOM product and altimetry. The spatial average of the difference map has been subtracted. The gray lines in the maps indicate the 1,000 and the 4,000-m isobaths from ETOPO1.

Boundary Current (Stommel & Arons, 1959). The dense waters that "leak" out of the boundary current can continue to flow equatorward through interior pathways, contributing to the dense southward limb of the Atlantic Meridional Overturning Circulation (AMOC) (Biló & Johns, 2019; Koelling et al., 2020; Xu et al., 2015). Further analyses with synthetic Lagrangian floats in high-resolution ocean circulation models have corroborated the evidence that interior pathways contribute to the total equatorward transport in the deep North Atlantic (Gary et al., 2011; Lozier et al., 2012). The curvature of the shelf-break creates hot spots of leakiness that can be observed in both Lagrangian and Eulerian frames of reference (Solodoch et al., 2020). Yet, temporal variability of this leakiness from the boundary currents into the interior has seldom been explored.

To investigate the circulation near the Tail of the Grand Banks using a model, it is important to choose a simulation that performs well in this complicated region. Ocean circulation models have historically failed to accurately simulate the Gulf Stream between Cape Hatteras and the Grand Banks. As will be described in Section 2, we use a Hybrid Coordinate Ocean Model (HYCOM) simulation that has been extensively validated against the surface and subsurface observational data in the North Atlantic, including crucial validation of the velocity field compared to transport mooring arrays (Gonçalves Neto et al., 2020; Xu et al., 2013, 2018).

In this study, we use Lagrangian analyses in this high-resolution ocean circulation model to better understand the circulation changes at the Tail of the Grand Banks that are associated with the rapid warming of the Northwest Atlantic Shelf and Slope after 2008. To do so, we deploy a suite of synthetic particles in the vicinity of the Labrador Current in the eastern Grand Banks and track their dispersion in a Lagrangian framework. We then contextualize the variability of the Lagrangian dispersion with an analysis of the accompanying Eulerian properties in the region.

2. Data and Methods

2.1. Numerical Model

This study is performed using outputs from a 1/12° simulation using the HYCOM of the North Atlantic Ocean (Xu et al., 2013). This HYCOM simulation, which did not assimilate observational data, has a hybrid vertical configuration with 32 layers that combines aspects of z-level and density coordinates (Bleck, 2002; Chassignet et al., 2003; Halliwell, 2004): Beneath the surface mixed layer, the model layers are nearly isopycnal; in the surface mixed layer, the model layers are isobaric. It is forced by the European Center for Medium-Range Weather Forecasts reanalysis ERA40 for 1978–2001 (Uppala et al., 2005) and by the Fleet Numerical Meteorology and Oceanography Center Navy Operational Global Atmospheric Prediction System for 2002-present (Rosmond et al., 2002). This Atlantic simulation has been shown to accurately represent important aspects of the shallow and deep circulation of the North Atlantic (Gonçalves Neto et al., 2020; Xu et al., 2013, 2018). In particular, this model faithfully represents the mean full-depth transport structure observed with moored instruments in the eastern Labrador Sea at 53°N and at the Tail of the Grand Banks at 43°N (Fischer et al., 2004, 2010; Schott et al., 2004). The original model output is available as daily averages for 1978–2017. The Lagrangian analysis described below is performed on the period between January 1993 and December 2017, the overlapping period between available model output and satellite altimetry. The final datasets used here are freely available (Gonçalves Neto et al., 2022).

As one illustration of the simulation's fidelity to observations, the spatial correlation between the HYCOM and the altimetry mean sea surface height fields is shown in Figure 2 is $R = 0.97$ ($p < 0.001$). The map of mean sea surface height from altimetry (Figure 2a) reveals a meridional gradient along the entire extent of the Gulf Stream between Cape Hatteras and the Grand Banks, with the ocean surface being higher to the south. South of the Grand

Banks, at 50°W, the Gulf Stream flows seaward of the 4,000-m isobath and takes a sharp northeastward turn. The Atlantic HYCOM captures these spatial patterns (Figure 2b) quite well, with a similar angle and mean position of the Gulf Stream path near the Tail of the Grand Banks. The modeled time-mean Gulf Stream jet downstream of the New England Seamount Chain is more diffuse (less energetic) than in observations, with a positive/negative bias in the northern/southern part of the Gulf Stream (Figure 2c). It was shown by Chassignet and Xu (2017) that this model feature is drastically improved when the horizontal resolution is increased from 1/12° to 1/50°, highlighting the importance of mesoscale and sub-mesoscale eddies in the energetics of the Gulf Stream extension.

Until recently, the inaccuracy of ocean models to simulate the Gulf Stream separation from the shelf break compromised their ability to depict the path of the Gulf Stream between Cape Hatteras and the Tail of the Grand Banks (Chassignet & Marshall, 2008). A recent inter-comparison of the Gulf Stream in 13 ocean reanalyses and unconstrained simulations showed that HYCOM outperformed other eddy-resolving, eddy-permitting, and coarse resolution models (Chi et al., 2018). Specifically, HYCOM had the best simulation of the Gulf Stream path and a number of metrics analyzed at the Oleander Line: maximum Gulf Stream velocity, 15°C isotherm position bias, mean Gulf Stream transport, as well as the highest correlation with observations in net transport and Gulf Stream latitude. It is important to note that the simulation used here is based on the HYCOM ocean model and includes the same temporal and spatial resolutions and vertical scheme, but does not assimilate data and was not the one used in the model inter-comparison described by Chi et al. (2018). Preliminary comparisons between the two versions of the model and observed altimetry data (not shown here) indicated that both are able to accurately simulate the sea surface height and surface velocity fields in the region. We chose to use this version of the model rather than the data-assimilating one because it has proven effective in simulating the subsurface velocity structure at the Tail of the Grand Banks, which is the focus of this study.

2.2. Lagrangian Analysis

Daily mean velocity fields from the HYCOM/Atlantic simulation are used to track the trajectories of synthetic particles launched from the launch site, shown in Figure 1. The synthetic particles were deployed and tracked in offline mode, which has the advantage of the reduced computational cost compared to running new simulations with online synthetic particles, using the open-source code OceanParcels (https://oceanparcels.org/) (Delandmeter & van Sebille, 2019; Lange & van Sebille, 2017) in Python.

HYCOM's hybrid vertical configuration allows for an isopycnal 2-D Lagrangian analysis, provided that the particles stay beneath the mixed layer during their entire path. While following isopycnals, the particle trajectory includes vertical motion where the isopycnal layer shoals or deepens, while drastically reducing the computational cost that a fully 3-D analysis would require. We chose to perform the Lagrangian analysis on the model Layer 19 because this layer contributes to the Slope Water and influences Northwest Atlantic Shelf properties, but is dense enough that, in the region studied here, it only outcrops in the shallowest parts of the shelf. We highlight, however, that the focus of the current Lagrangian Analysis is, primarily, to determine the direct influence of the Labrador Current on the continental slope, where the Slope Water is formed. The composition of the Slope Water is, in turn, responsible for shelf temperature fluctuations through deep channels connecting the continental slope to the Gulf of Maine (Northeast Channel) and the Gulf of St. Lawrence (Laurentian Channel) (Fratantoni & Pickart, 2007; Lauzier, 1965; Ramp et al., 1985). When the Slope Water is composed of less cold Labrador waters relative to warm subtropical waters, as it has since 2008 (NFSC, 2021), this composition shift contributes to the warming of the shelf.

Most of the analyses presented here were repeated on Layer 20 and had similar results. While this work focuses on relatively shallow layers that may influence the Slope and Shelf water variability, similar analyses on the Labrador Sea Water (Layers 21–24) and the Denmark Strait and Iceland-Scotland Overflow Waters (Layers 25 to bottom), though outside the scope of this paper, could provide insights on the variability of the lower limb of the Atlantic Meridional Overturning Circulation in the Northwest Atlantic.

The typical potential density of Layer 19, as referenced to 2,000 dbar, is $\sigma_2 = 36.52$ kg m^{-3}, with a mean temperature of 6.45°C and salinity of 34.44 in the study region. The model works on σ_2 coordinates, and its typical value for Layer 19 is approximately equivalent to $\sigma_\theta = 27.53$ kg m^{-3} at its mean depth of 587 m (Figure 3). This layer is isopycnal in 78.2% of the grid points over the study region shown in Figure 2 and over all time analyzed (years 1993–2017). The layer outcrops in 19.2% of the grid points, which corresponds to the majority of the continental shelf in the region; here, the surface waters are denser than those represented by Layer 19, so the layer essentially

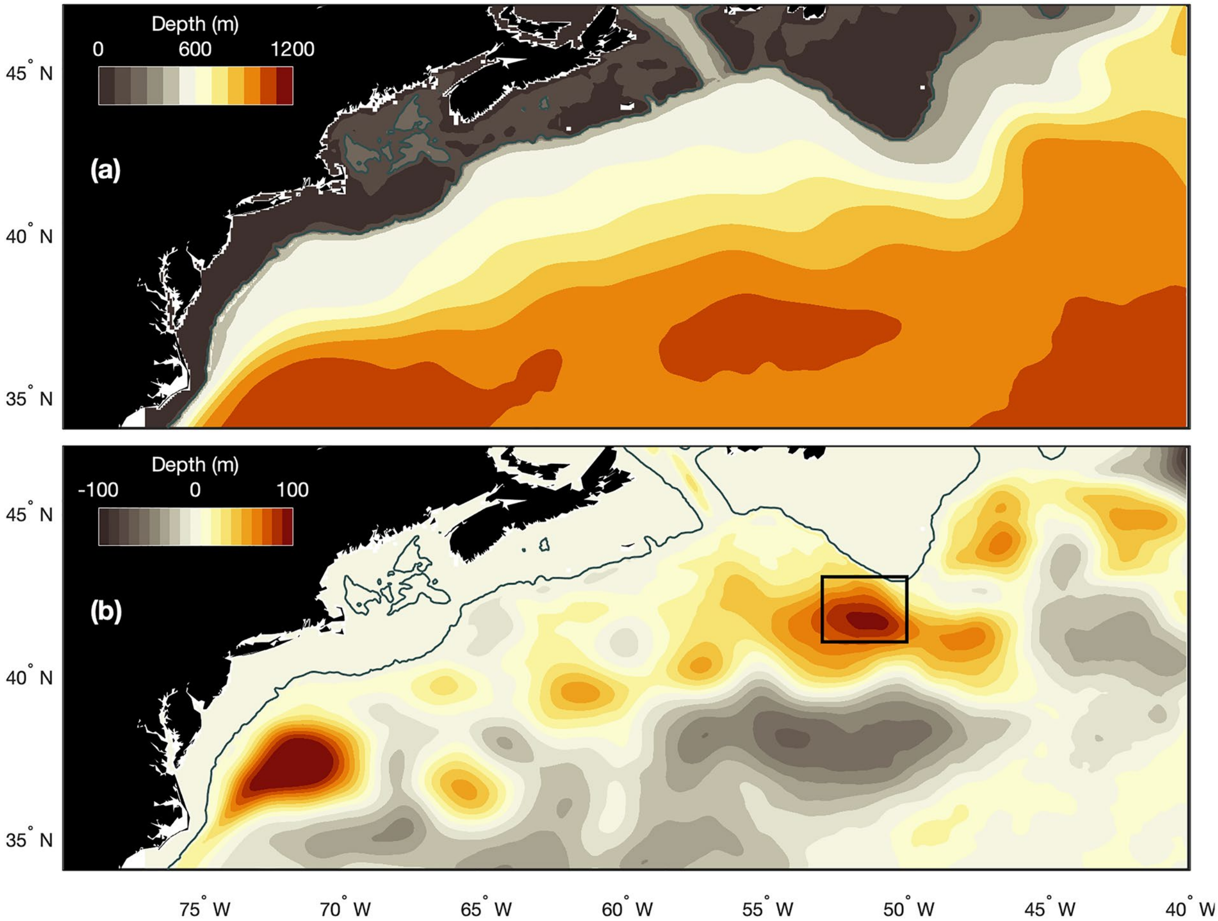

Figure 3. (a) Mean depth of model layer 19, on which the Lagrangian particles travel. Layer 19, which has typical sigma-2 = 36.52 kg m^{-3} in the ocean interior, is similar to sigma-θ = 27.53 kg m^{-3}. Where the layer depth is zero, the surface waters are as dense or denser than those represented by Layer 19. (b) Difference in the depth of Layer 19 averaged over the period after 2008 minus the average over the period before 2008. Positive numbers reflect the deepening of this layer.

vanishes. Layer 19 behaves as an isobaric mixed layer in only 2.5% of the grid points, mostly corresponding to the area northeastward of the Grand Banks. Layer 19 is shallowest along the continental slope, varying from about 300 m in the eastern Grand Banks to 500 m in the Mid-Atlantic Bight. Its thickness is the largest ($H \geq 80$ m) along the slope between the Tail of the Grand Banks and the Scotian Slope (50°W to 60°W), and farther offshore on the eastern side of the Grand Banks, between 50°W and 40°W.

Figure 3a shows the mean depth of Layer 19. Note that where the plotted depth is zero, the mixed layer is as dense or denser than Layer 19. Figure 3 shows that Layer 19 plunges to below 1,000 m in the thermocline of the Gulf Stream and subtropics, it shoals to between 200 and 500 m shoreward of the Gulf Stream in the Slope Sea, and it outcrops on the shelf. The layer depth also varies over time. During the period following 2008, Layer 19 deepened close to the continental slope and shoaled further offshore relative to the period before 2008 (Figure 3b), consistent with a shift of the Gulf Stream or its eddies toward the shelf.

The synthetic particles were deployed in Layer 19, in the vicinity of the Labrador Current on the eastern flank of the Grand Banks (in every grid cell from 45.5°N, 48.5°W to 45°N, 48°W) between January 1993 and December 2016 and tracked forward in time for 1 year using the fourth-order Runge-Kutta scheme (Dormand & Prince, 1980). This method interpolates the velocity field between consecutive time-steps and therefore is suitable for offline Lagrangian analyses performed at daily (or longer) temporal resolution (van Sebille et al., 2018). Eighty particles were simultaneously deployed every 10 days, totaling nearly 75,000 particles deployed over 24 years. Following the method described by Jones et al. (2016), sensitivity analyses were performed with identical experiments with 20 and 40 simultaneously-deployed particles at the same location to assure that the run with 80 particles was robust, and the results in both cases were statistically indistinguishable from the ones presented below.

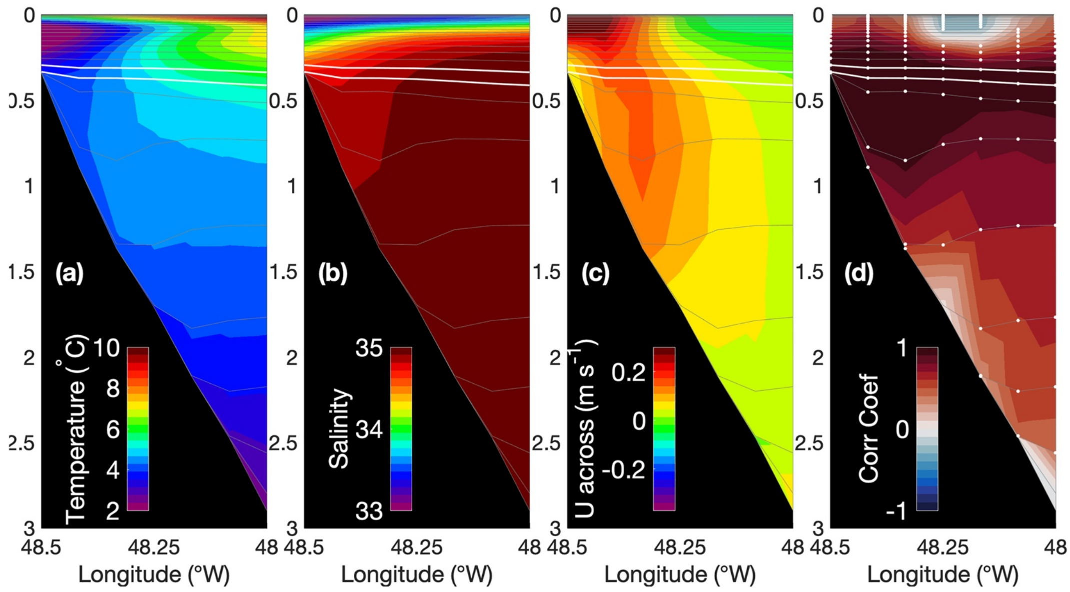

Figure 4. Cross-section of a 10-year (2003–2012) mean (a) temperature, (b) salinity, (c) velocity, and (d) correlation coefficients between the velocity at Layer 19 and the velocity at every layer at the launch site, in the eastern Grand Banks. The velocity is normal to the section and has been rotated from the original zonal and meridional components, with positive values in the direction of the mean flow of the Labrador Current (i.e., southwestward). In panel (d), the correlation coefficients were calculated between the time-varying cross-sectional model velocity at each grid point of Layer 19 and that at every model layer at that grid point. The model grid points where the correlation is statistically significant at the 99th percentile are identified with white dots. The boundaries between the model layers are shown in thin, gray contours, with Layer 19 highlighted with thick, white contours. The section is 68-km long (x-axis), with the continental shelf to its left and the open ocean to its right. Lagrangian particles were deployed in every grid point in Layer 19 along this section. Contour intervals of temperature, salinity, and velocity are, respectively, 0.1°C, 0.025 and 0.01 m s^{-1}.

2.3. Properties of the Lagrangian Launch Site and Mean Trajectories

The release location was chosen because it is immediately downstream of the region where, on average, the branches of the Labrador Current on either side of the Flemish Cap converge. Previous Lagrangian simulations showed that only a small portion of particles launched in the Labrador Current upstream of Flemish Cap remains in the current all the way to the Tail of the Grand Banks (Bower et al., 2011). By launching south of Flemish Cap, we ensure that most particles reach the Tail of the Grand Banks.

Figure 4 shows the time-mean section where the particles were released. The Labrador Current skirts the shelf-break, with a surface-intensified core centered over the 500-m isobath and a deeper, more uniform core over the 1,500-m isobath. The mean southwestward flow extends to the seafloor with the Labrador Sea Water centered between 500 and 1,000 m. In the top two hundred meters, the Labrador Current is flanked farther offshore by the northeastward-flowing waters of the meandering North Atlantic Current. The characteristic low temperature and salinity of the Labrador Current are evident in the mean cross-section. Layer 19 is located at the top of the deeper jet and on average is moving southwestward across the entire section shown in Figure 4.

Throughout the domain analyzed in this study, this layer is located immediately above the Labrador Sea Water (Xu et al., 2013). Transport on Layer 19 is likely representative of the deeper, offshore branch of the Labrador Current, since its upper branch, which can migrate onto the shelf itself, is contained in shallower layers in the more stratified upper ocean. In fact, the velocity at model layers 15–22 is significantly correlated with that at Layer 19 at the launch site (Figure 4d). At least at this location, all of the southward velocities along the slope of the Grand Banks are positively correlated, therefore corroborating the use of Layer 19 as a proxy for Labrador Current velocity. Though beyond the scope of the current study, it would be interesting to explore whether transport in the Deep Western Boundary Current, containing the densest components of North Atlantic Deep Water correlate with transport variability in the Labrador Current.

The mean temperature, salinity, velocity, and thickness of Layer 19 at the launch site cross-section are, respectively, 4.96 ± 0.41°C, 34.91 ± 0.04, 7.8 ± 4.9 m s^{-1} and 63.9 ± 7.8 m, where the uncertainty is one standard

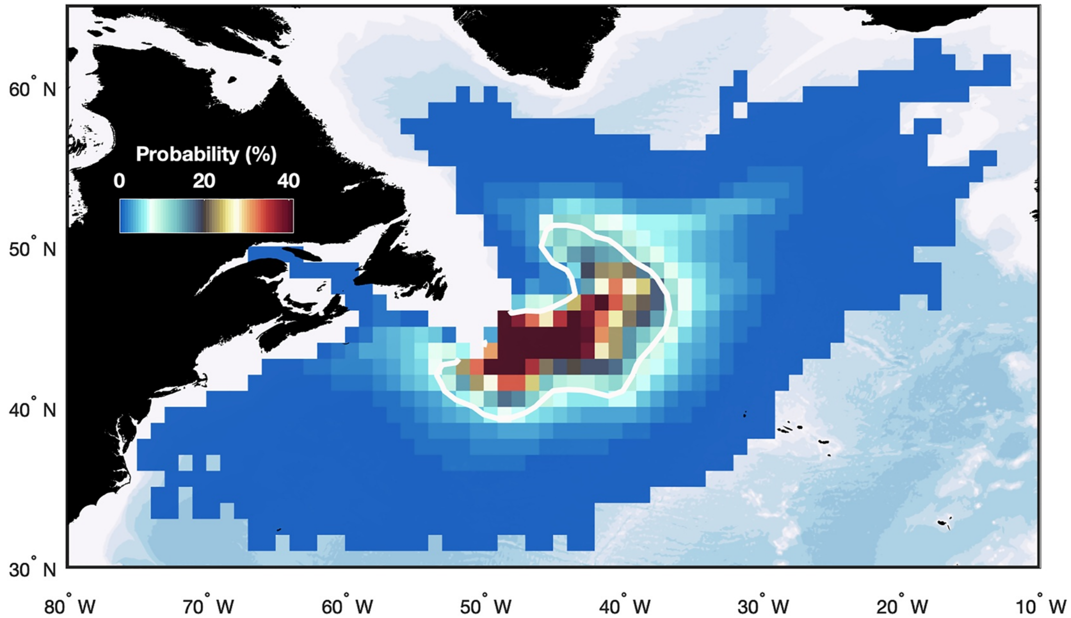

Figure 5. Probability distribution map of synthetic particles tracked for 1 year after deployment at launch site from 1993 to 2016, calculated at 1° × 1° bins. The white contour shows the 10% probability contour. The bathymetry is shown where the probability is equal to zero.

deviation of the monthly means. Interannual variability from 1993 to 2017 in Layer 19 at the launch site is smaller than on the shelf, with annual mean temperature and salinity ranging from minimums of 4.32 ± 0.40°C, 34.86 ± 0.06 in 1994 to maxima of 5.32 ± 0.243°C and 34.94 ± 0.02 in 2000 and 2011, respectively.

3. Results and Discussion

3.1. Mean Lagrangian Trajectories

The Lagrangian analysis of the synthetic particles provides information on the circulation near the Tail of the Grand Banks. In the 10 days immediately following deployment, 89% of the particles flowed southward toward the Tail of the Grand Banks. The remaining 11% of the particles that initially flowed northward were mostly deployed on the offshore edge of the cross-section and likely associated with the meandering of the North Atlantic Current close to the shelf-break. Subsequently, the 1-year trajectories of the particles launched between 1993 and 2016 were highly dispersive and filled a great area of the Subtropical and Subpolar North Atlantic (Figure 5), similar to the results of observed and modeled Lagrangian trajectories shown in Bower et al. (2011). The mean probability map indicates that, within 1 year of deployment, some synthetic particles reached distant areas, such as the Iceland Basin and central subtropical gyre. The 10% probability contour in Figure 5 encircles the two most typical paths: The westward propagation along the southern edge of the Grand Banks, and the northeastward propagation along the North Atlantic Current. The direct pathway to subtropical latitudes (south of approximately 40°N) via interior pathways is also apparent around a longitude of 50°W.

Although the particles typically departed southward along the shelf-break upon deployment, the vast majority of them were ejected from the Labrador Current near the Tail of the Grand Banks and ended their 1-year journey to the northeast (45.6%, 12,028 particles) or southeast of the launch site (38.4%, 10,123 particles). Only 3,759 particles (14.3%) were found southwest of the launch site 1 year after deployment. Furthermore, the shape of the distribution map suggests that the particles that flow northeastward tend to travel farther than those flowing southwestward.

3.2. Seasonal Variability of the Lagrangian Trajectories

The probability distribution maps have a strong seasonal cycle (Figure 6a). The particles deployed in the spring and summer (March-August) are more likely to turn toward the northeast upstream of the Tail of the Grand Banks

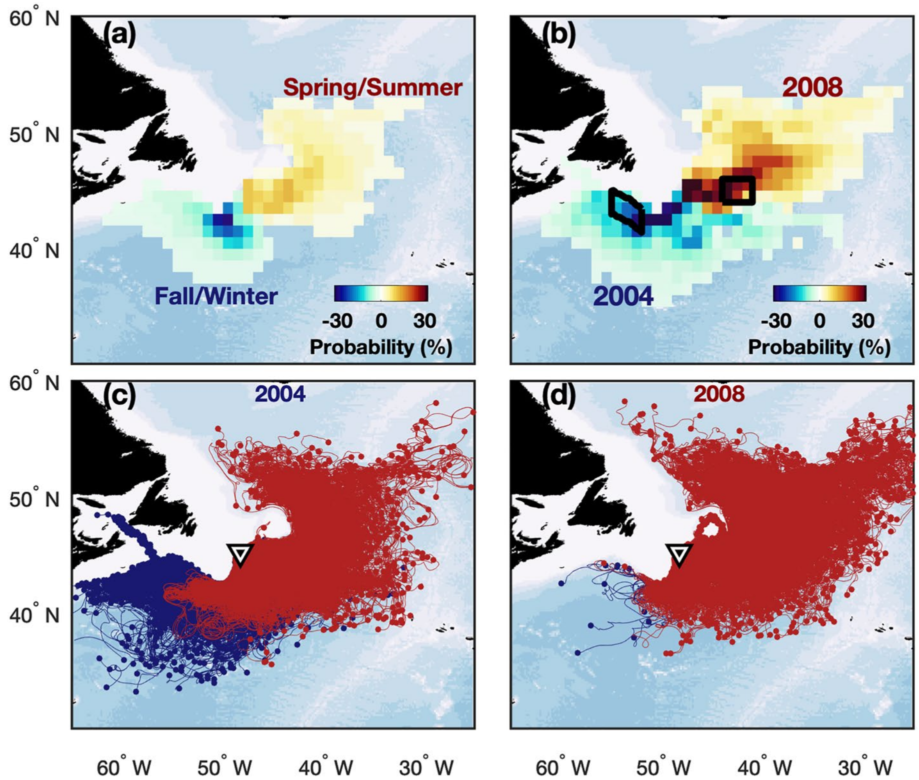

Figure 6. (a) Difference in the probability distribution of synthetic particles deployed between March and August (Spring/Summer) minus those deployed between September and February (Fall/Winter) and tracked for 1 year, calculated at $1° \times 1°$ bins. (b) Same as (a), but for particles deployed in 2008 minus particles deployed in 2004. The Slope and NAC boxes are identified in black. In panels (a) and (b) the grid points whose difference was between -1% and 1% are masked out. (c) One-year trajectories of Slope (blue) and NAC Particles (red) that were launched in 2004, defined as the particles that were sampled in the regions shown as black polygons in panel b. (d) Same as (c), but for those particles launched in 2008. The definition of Slope and NAC Particles was the same for both years. In 2008, only 34 particles met the criteria of entering the Slope Region less than 3 months after being deployed in the 10-day Lagrangian tracking output.

and to travel farther distances along the path of the North Atlantic Current. Conversely, the probability map of the fall and winter (September-February) deployments indicates that more of these particles follow the Labrador Current westward along the southern edge of the Grand Banks. The seasonality in the probability distribution of particles aligns with seasonality in the velocity of the Labrador Current at the launch site: higher Labrador Current velocities at the launch site in the Fall and Winter are coupled with higher fractions of particles flowing along the Labrador Current past the Tail of the Grand Banks. Similarly, lower velocities at the launch site in the Spring and Summer are associated with higher northeastward transport of particles to the North Atlantic Current.

The seasonality of the upstream Labrador Current transport at the launch site is evident in both observational and other modeling studies. Both show that the Labrador Current is typically stronger in the Fall/Winter and weaker in the Spring/Summer between the bifurcation that feeds its inshore branch and the Tail of the Grand Banks (Han et al., 2008; Wang et al., 2015). In the Spring/Summer, the Gulf Stream sheds more warm core rings (Silver et al., 2021), which could affect the continuity of the Labrador Current at the Tail of the Grand Banks. Therefore, seasonality in the Gulf Stream eddy generation and Labrador Current transport could contribute to the seasonality observed in the Lagrangian trajectories described above.

3.3. Interannual Variability of the Lagrangian Trajectories

3.3.1. Two Contrasting Years of Lagrangian Trajectories

These Lagrangian trajectories vary dramatically from year to year. The clearest difference occurred for the particles launched in 2004 compared to 2008. In 2004 more particles were moving westward along the shelf-break, as compared to more particles moving northeastward along the North Atlantic Current in 2008 (Figure 6b). We expect the distinct behavior of particles in 2008 versus 2004 to result in a decrease of particles that reach the Scotian Slope.

To identify the particles that flow along the shelf-break toward the Scotian Slope, a terrain-following box is defined in Figure 6b as the Slope Region. This box is defined between 52°W and 55°W, is bounded by the 1,000-m isobath to the north, and extends 2° of latitude to the south. The particles that were sampled within this box at least once during the first 3 months following deployment were considered slope particles (blue lines, Figures 6c and 6d). The timing is determined based on the result that the particles that follow the Labrador Current along the shelf-break generally take 2 to 3 months to round the Tail of the Grand Banks and enter the slope region. The longitude band (52°W to 55°W) was chosen to avoid accounting for particles that are swept eastward in the Gulf Stream just to the west of the Tail of the Grand Banks, near 51°W.

During the 25-year output analyzed here, only 13.0% of the 70,195 particles are Slope Particles. However, the fraction of particles that meet the Slope criteria varies considerably between years, ranging from greater than 36% in both 1998 and 2004 to less than 1.1% in 2007 and 2008. In the latter years, only 55 out of 5,840 particles were Slope Particles. In addition to the stark difference in the number of particles that make it to the Slope Region, the behavior of the Slope Particles is also very different between these two periods. In 2004, for example, Slope Particles are found throughout most of the Slope Region between the Western Grand Banks and the Northeast Channel, and invaded the Gulf of St. Lawrence. A small number of particles is observed farther offshore, possibly exported from the Slope Region by mesoscale activity. In 2008, only 34 particles were classified as Slope Particles, and these never traveled west of 60°W, just offshore of the Laurentian Channel.

Although this distinct behavior could arise due to the reduced number of particles in 2008, it is noteworthy that such a large difference has consequences for shelf warming in the latter year. In fact, this causality is further confirmed by the lagged correlation coefficients between the percentage of Slope Particles (blue bars in Figure 7b) and the temperature at Layer 19 along the Scotian Shelf between the Laurentian Channel and the Gulf of Maine. The maximum correlation was $R = -0.52$ ($p < 0.001$) with the Slope Particles leading by 3 months. The negative correlations indicate that an increase in the number of Slope Particles is associated with colder temperatures in the Scotian Shelf, as anticipated.

To track a common alternative pathway, we defined a second region south of Flemish Cap, which we call the NAC Region, as a reference to the North Atlantic Current (Figure 6b). The particles that were sampled within this box at least once are called NAC Particles (Red lines, Figures 6c and 6d). Overall, 65.0% of the particles meet the NAC Particle criteria, ranging from 38.6% in 2004% to 82.4% in 2008. These statistics show that 2004 experienced high connectivity of the Labrador Current around the Tail of the Grand Banks to the Scotian Shelf, but that pathway was almost entirely blocked in 2008, during which a much greater portion of the particles following the eastward pathway of the North Atlantic Current.

3.3.2. An Eulerian View of the Interannual Variability of the Lagrangian Trajectories

Next, we explore the dynamics driving the variability of the particle trajectories at the Tail of the Grand Banks. To do so, we use the concept of the potential thickness (Figure 7). Conservation of angular momentum constraints a water parcel of a given potential density to travel along contours of a potential thickness of that density layer, in the absence of any external input of vorticity, like from wind stress curl. The potential thickness is defined as the depth between two isopycnal layers, normalized to a reference latitude: $H = \frac{f \times (D_{lower} - D_{upper})}{f_{ref}}$ where f is the Coriolis parameter, D_{lower} is the depth of the lower bounding isopycnal (or the sea floor), D_{upper} the upper bounding isopycnal (or the sea surface), and f_{ref} is the Coriolis parameter at a reference latitude.

Layer 19 is at the base of the pycnocline, and therefore sits at the top of the less stratified, deep limb of the Labrador Current (Figure 4). We propose a conceptual model of a two-layer ocean, with Layer 19 part of a cold, deep layer, situated beneath a warmer upper layer. Using the equation above, we define the potential thickness of the deeper layer as the depth between Layer 19 and the seafloor, normalized to 40°N. The offshore branch of the Labrador Current at the Lagrangian particle launch site travels over deep bathymetry, where the mean potential thickness of the deep layer (i.e., below Layer 19) is 2,300 m (Figure 6).

On average, the 2300 m potential thickness contour continuously hugs the slope of the Grand Banks from the Lagrangian launch site, around the Tail, and to the Scotian Slope (Figure 7a). Therefore, a reasonable hypothesis

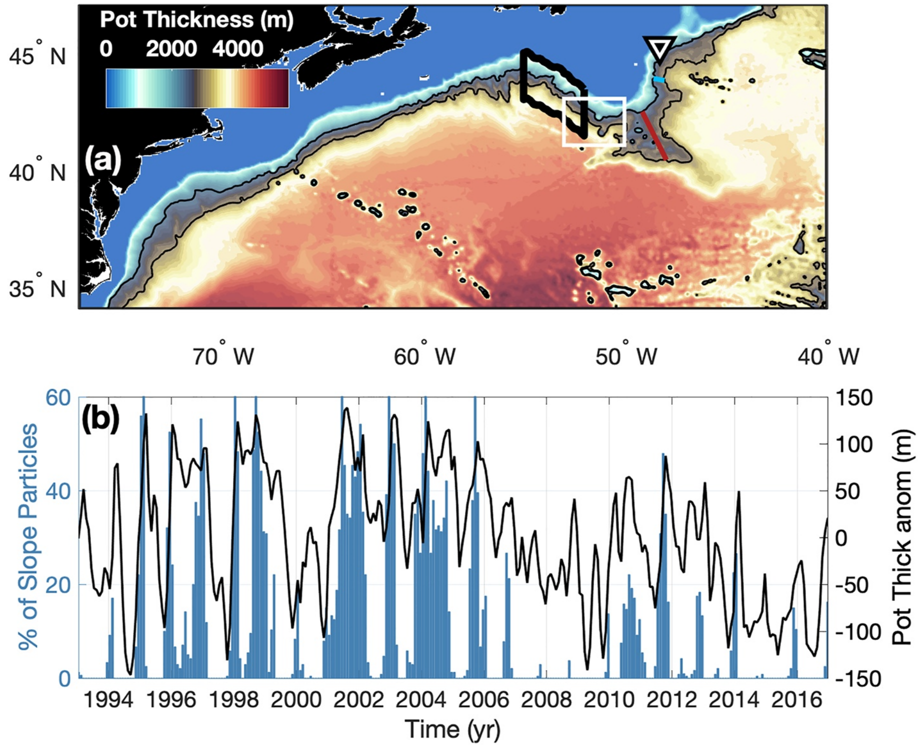

Figure 7. (a) Mean potential thickness from Layer 19 to the bottom of the ocean. The Slope Region is outlined by a thick black box and the launch site is identified as a black and white triangle. The 2,300-m and the 3,000-m mean potential thickness contours are shown as thin black lines. The blue and red lines are used to calculate the distance between the 2,300 and 3,000-m mean potential thickness contours at the launch site and at the Tail of the Grand Banks, respectively. The white box is used to calculate the potential thickness anomaly shown in panel b. (b) Monthly percentage of particles reaching the Slope Region within 3 months of launch (blue bars), plotted as a function of the date of launch between Jan 1993 and Dec 2017, and monthly potential thickness anomaly at the Tail of the Grand Banks (black line, averaged over white box in panel a and black box in Figures 10a and 10b, 10c). The two time series have the highest correlation coefficient when the Tail of the Grand Banks potential thickness anomaly lags by 1 month ($R = 0.70$, p-value < 0.001).

would be that a large number of Lagrangian trajectories would follow this contour without interruption. However, this eddy-rich region (Brickman et al., 2018; Solodoch et al., 2020) experiences large fluctuations of potential thickness along the slope. Indeed, the monthly potential thickness averaged over a box on the southwest edge of the Grand Banks can fluctuate by more than ±100 m (black line in Figure 7b). When the lower layer is squashed (i.e., negative thickness anomalies), very few Lagrangian particles are able to make the journey to the Scotian Slope (blue bars in Figure 7b).

In our 2-layer conceptual framework, the Labrador Current particles would migrate downslope (i.e., offshore) to maintain their potential thickness in the presence of the deepened pycnocline and squashed lower layer. Once they are further offshore, the particles are more likely to be swept eastward with the North Atlantic Current. Though potential thickness contours between 2,300 and 3,000 m are extremely bunched together at the launch location, they spread much further at the actual Tail of the Grand Banks, as emphasized with a red line in Figure 6. Given the variable potential thickness gradient, a particle experiencing a 200 m potential thickness anomaly would need to migrate nearly 70 km offshore to maintain its path on a constant potential thickness contour at the Tail of the Grand Banks (as opposed to only 10 km at the launch site along the blue line). The snapshots in Figure 7 show mesoscale features that are somewhat smaller than the averaging box used to create Figure 6b. These mesoscale eddies frequently squash the lower layer by more than 200 m, leading to particle excursions far offshore where they are vulnerable to being entrained in the North Atlantic Current.

On average, only 13.0% of the particles reached the Slope Region within 3 months after being deployed. But there is high variability: transport to the Slope Region exceeded 40% in several months and was completely cut off in others (Figure 7b). In particular, the highest Lagrangian connectivity was seen in 2003–2004, associated

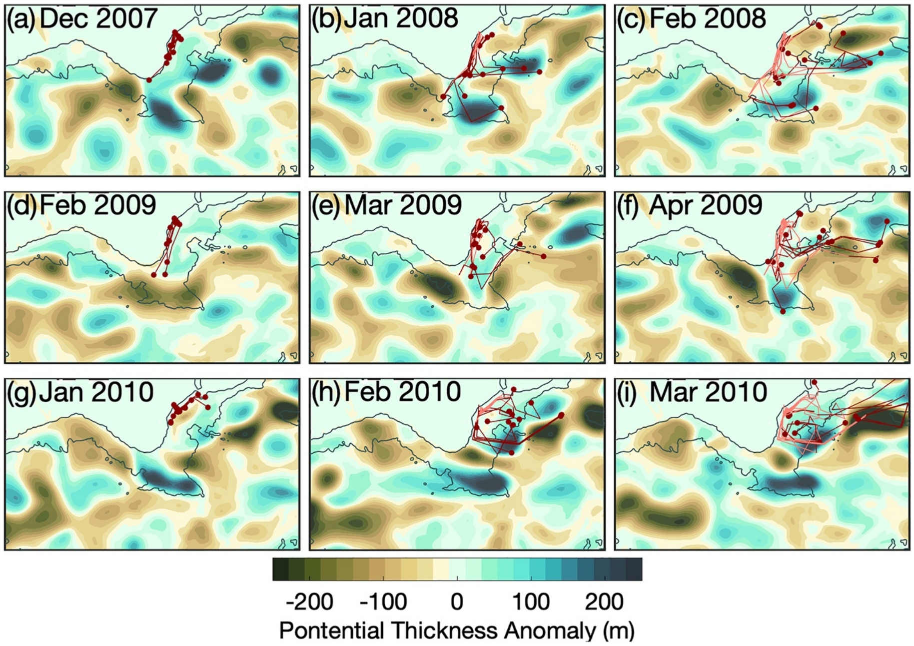

Figure 8. Potential thickness anomaly on three selected months with no slope particles, tracked for three consecutive months. Each row represents one event: (top) Dec 2007, (middle) Feb 2008, and (bottom) Jan 2010. The columns show the progress of each event from (left) the month of deployment to (right) 2 months after the deployment. In each map, the trajectories of 15 randomly-selected particles are shown. The trajectory of each particle in a given month is shown in dark red and the trajectory in the previous one (middle column) or 2 months (right column) is shown in salmon. The 1,000 and 4,000-m isobaths are shown in thin black contours.

with positive potential thickness anomalies at the Tail of the Grand Banks (Figure 7b). Similarly, the low rates in 2007–2008 occur during negative potential thickness anomalies. The two time series are significantly correlated, with the highest correlation coefficient when the month in which the particles are released leads by 1 month ($R = 0.70$, p-value < 0.001). We conclude that the potential thickness anomaly at the Tail of the Grand Banks 1 month after the release of the particles is tightly related to the continuity of the Labrador Current.

We have shown that the layer thickness anomalies and the Labrador Current trajectories are related, but the sign of this potentially causal connection is not yet clear. To address this, we provide snapshots of the layer thickness anomalies as the trajectories approach the Tail of the Grand Banks (Figure 8). This figure shows three examples of 3-month periods during which no particles reached the Slope Region for a given deployment month. These periods illustrate the various locations at which Labrador Current particles can be steered offshore by the Gulf Stream or its eddies. Here, the colors represent the potential thickness anomaly, that is, the deviation of the potential thickness from the mean field shown in Figure 7a. The negative values indicate the deepening of Layer 19, associated with the squashing of the bottom layer and stretching of the upper layer. These events are associated with anticyclonic Gulf Stream meanders and eddies. Alternatively, the positive values indicate the shoaling of Layer 19, the thickening of the bottom layer, and thinning of the upper layer, associated with cyclonic anomalies that accelerate the along-slope velocities at the Tail of the Grand Banks. With no exceptions, the particles that are swept away from the shelf-break and transported to the northeast at or upstream of the Tail of the Grand Banks during these months always do so on the eastern flank of an anticyclonic meander/eddy (i.e., to the right of the brown shades in Figure 8).

The three examples of Labrador Current blocking shown in Figure 8 shed light on the various events that can lead to the offshore transport of particles deployed in the Labrador Current. In December 2007 (Figure 8a), the only large anticyclonic anomaly impinging on the shelf-break was on the western flank of the Grand Banks. The particles deployed early in that month quickly reached the Tail of the Grand Banks. Then, in January 2008 (Figure 8b), the particles that were already at the Tail of the Grand Banks were steered offshore; simultaneously, a second anticyclonic anomaly approached the shelf-break at the eastern flank of the Grand Banks and blocked the particles that were deployed in late December. By February 2008 (Figure 8c), all of the particles deployed in December 2007 had been ejected from the Labrador Current in two locations by two different anticyclonic anomalies.

10.1029/2022JC018756

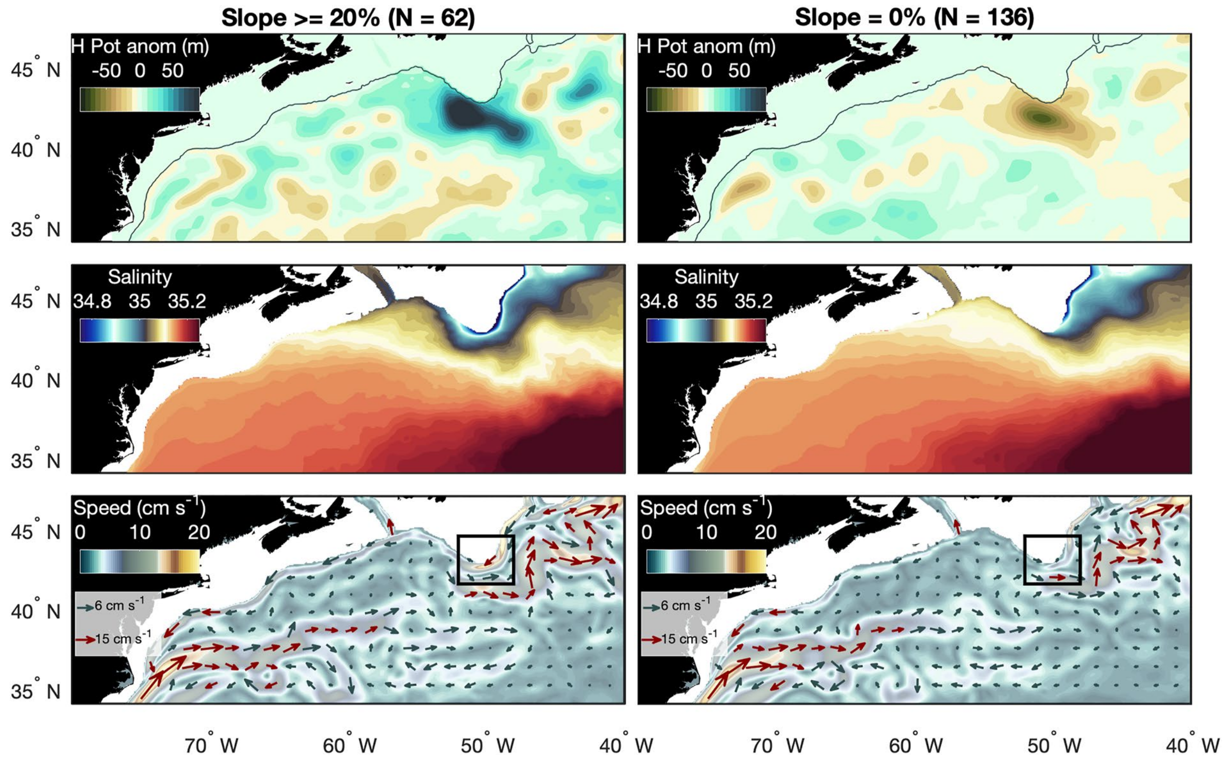

Figure 9. Composite averages of (a), (b) potential thickness below Layer 19, (c), (d) salinity on Layer 19 and (e), (f) mean velocity of Layer 19. The panels on the left show periods of strong Labrador Current connectivity: they are averaged for months in which 20% or more of the particles reached the Slope Region within 3 months. The right hand panels are for months in which no particles reached the Slope Region. The averages are calculated during the second month after deployment. The black contour in panels (a) and (b) shows the 1,000-m isobath. The black box in panels (e), (f) is centered at 43°N, 50°W.

The blocking of the Labrador Current and consequent transport of particles along the pathway of the Gulf Stream and/or the North Atlantic Current may occur at (Figures 8d–8f), downstream (Figures 8a and 8b), or upstream of the Tail of the Grand Banks (Figures 8g–8i). The different scenarios in which Labrador Current particles are blocked are shown in Figure 7 shows how water parcels face an "obstacle course" of anticyclonic eddies that can knock them off their path in the boundary current at the Grand Banks. This result is in line with the trajectories of 700 and 1,500 m RAFOS floats deployed and tracked by Bower et al. (2011), which showed that anomalous positive mean dynamic topography corresponded with anticyclonic circulation capable of diverting floats out of the boundary current and transporting them toward the east.

We refer to months when the Labrador Current carries at least 20% of its particles continuously westward past the Tail of the Grand Banks to the Slope Region as Open Valve periods and months when no particles make the journey within 3 months of release as Closed Valve periods. From these criteria, composites are shown in Figure 9, made from the averages of the second month after deployment, which is approximately the time when the particles arrive at the Tail of the Grand Banks. The composites of potential thickness anomalies (Figures 9a and 9b) confirm that the Closed Valve is associated with a squashed bottom layer, with the negative potential thickness anomaly centered at the western flank of the Tail of the Grand Banks. The salinity (Figures 9c and 9d) and thickness of Layer 19 (Figure 10d) reflect changes in the continuity of the Labrador Current: the cold and fresh tongue that extends from the western Grand Banks to the Scotian Slope during Open Valve periods vanishes during Closed Valve periods, influencing much of the Slope Sea. Finally, the squashing of the deep layer is easily related to an increase in sea surface height anomalies (Figure 10a). Therefore, the two-layer conceptual framework mechanistically explains the previously observed correlation between satellite-observed sea surface height at the Tail of the Grand Banks and temperatures on the Northwest Atlantic slope and shelf (Gonçalves Neto et al., 2021).

The Open and Closed Valve composite velocity fields also reveal subtle changes in the mean circulation (Figures 9e and 9f). For instance, precisely at the southern tip of the Grand Banks, the composite average flow during Open Valve periods is directed southwest, allowing particles to round the Tail of the Grand Banks and

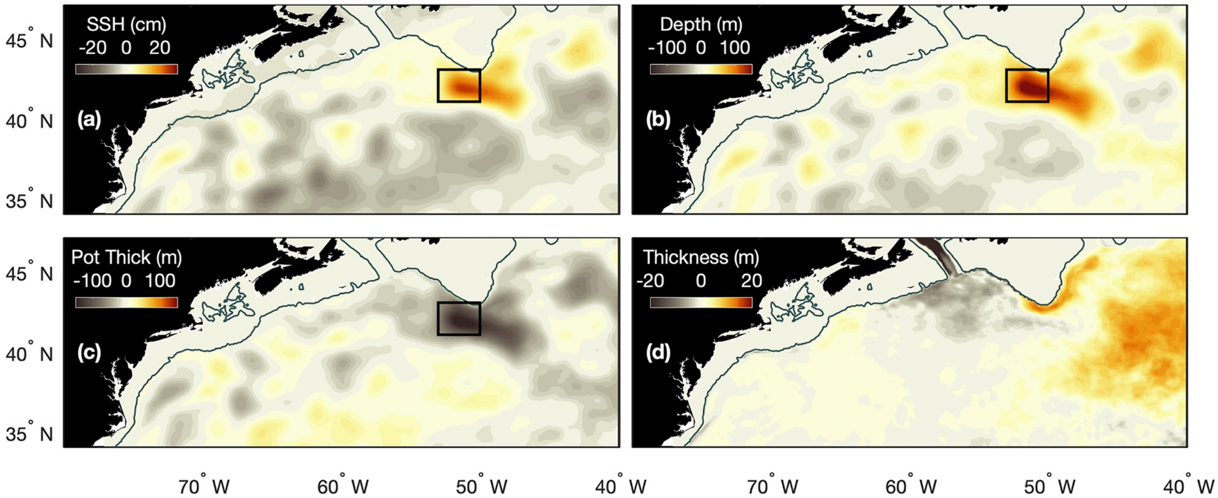

Figure 10. Difference between the closed valve months with no slope particles and the open valve months with 20% or more Slope Particles. (a) Sea surface height, (b) depth of Layer 19, (c) potential thickness between Layer 19 and the bottom and (d) thickness of Layer 19. The 200-m isobath is shown in black to show the approximate position of the shelf break.

continue to the Scotian Slope (see arrows inside the box at approximately 43°N, 50°W in Figure 9e). During Closed Valve months, the average velocity at this location is directed to the east, associated with a slight northward shift in the Gulf Stream.

In two follow-up Lagrangian experiments, we deployed particles in the Closed Valve and Open Valve composite mean velocity field. The particles advected in the mean Closed Valve velocity field were still entirely unable to reach the Slope Box. Perhaps more interesting, when particles were deployed in the Open Valve mean velocity field, *a lower proportion* (30%) of them reached the Slope Region than when they were deployed in the full, eddy-rich velocity field (40%). This result is opposite that of a Lagrangian model experiment by Bower et al. (2011), who found greater connectivity of the southwestward flow around the Tail of the Grand Banks for particles launched in the mean flow relative to the time-varying velocity field. Their experiments differed in the ocean circulation model used (1/12° FLAME model), the years represented (1994–1998), and the depth at which the particles were deployed (700 and 1,500 m). It is unclear to what degree these methodological differences are responsible for the differences in our results. However, we note that the active role of eddies in facilitating the transport of cold, fresh, oxygen-rich water around the Tail of the Grand Banks is consistent with the model analysis of Brickman et al. (2018), and is visually apparent in a richly-eddying model simulation of Claret et al. (2018) (see their supplementary video of oxygen concentrations).

4. Conclusions

A recent observational study (Gonçalves Neto et al., 2021) showed that an abrupt shift to a higher mean sea level at the Tail of the Grand Banks in 2008 preceded rapid subsurface warming that propagated along the Northwest Atlantic Slope between the Gulf of Saint Lawrence and the Gulf of Maine in 2009 and 2010. The Labrador Current feeds the Slope Water with cold water, so a decline in its westward transport past the Grand Banks directly contributes to the warming of the Northwest Atlantic Slope. The subsequent shelf warming is expected as the Slope Water invades the Gulf of St. Lawrence and the Gulf of Maine through the Laurentian Channel and the Northeast Channel, respectively (Fratantoni & Pickart, 2007; Lauzier, 1965; Ramp et al., 1985). This chain of events helps explain the shelf warming (Figure 1) following the 2008 “closing of the valve” at the Tail of the Grand Banks (Figure 7).

In this study, we performed a Lagrangian analysis in a high resolution ocean circulation model to explore the mechanisms responsible for the substantial interannual variability in the coherence of the Labrador Current at the Tail of the Grand Banks. The analysis of more than 75,000 synthetic particles suggests that the impingement of Gulf Stream meanders and eddies on the shelf-break at or near the Tail of the Grand Banks can completely cut off the Labrador Current, as they often did after 2007 in the simulation. The simulated Lagrangian analysis

10.1029/2022JC018756

described here provides a mechanistic explanation for this event: the strong positive sea surface height anomalies at the Tail of the Grand Banks, observed by satellite altimetry and simulated by the HYCOM model (Figure 10a), are associated with anticyclonic Gulf Stream meanders and eddies that completely block the Labrador Current.

These anticyclones are characterized both by the doming of the sea surface and the deepening of the pycnocline, illustrated by the increase of the depth of model Layer 19 (Figure 10b). Picturing the water column as a two-layer system, the deepening of the interface between the two layers implies the squashing of the bottom layer (Figure 10c). At the Tail of the Grand Banks, the deepening of the pycnocline decreases the potential thickness of the bottom layer. To conserve angular momentum the Lagrangian particles follow potential thickness contours and are therefore steered downslope/offshore when Gulf Stream meanders or eddies impinge on the slope of the Grand Banks. The offshore transport disrupts the along-slope continuity of the Labrador Current.

The stability of the Gulf Stream has been explored in studies using observations and models. According to a highly idealized eddy-resolving model (Spall, 1996), interactions of the Gulf Stream and Deep Western Boundary Current at Cape Hatteras can lead to oscillations between a stable and a meandering state of the Gulf Stream on a nearly-decadal time scale. The latter state is responsible for increased eddy generation that drives the formation of the northern recirculation gyre and eventually reaches the Tail of the Grand Banks. The intrinsic variability of the Gulf Stream stability and the consequent eddy generation are in turn controlled by the interaction between the Gulf Stream and the underlying North Atlantic Deep Water at Cape Hatteras.

More recent observational studies have documented subtle changes in the Gulf Stream circulation that may be linked to its shifting behavior at the Tail of the Grand Banks. First, between the New England Sea Mounts (near 70°W) and the Grand Banks, the Gulf Stream was likely weaker after 2010 compared with the 1980s, with a particular weakening of the cyclonic flank to its north, in the Slope Sea (Andres et al., 2020). Its destabilization point has also migrated westward, with a surge in Gulf Stream troughs and deep cyclones at Line W since 2008 (Andres, 2016), while its mean latitude has migrated northward since 2010 (NFSC, 2021). The increased destabilization of the Gulf Stream and the weakening of its recirculation could have allowed for more eddies reaching the shelf-break at the Tail of the Grand Banks and consequently decreased the connectivity of the Labrador Current to the Northwest Atlantic.

In the same period, there was an increase in the interior transport of North Atlantic Deep Water (2010–2017 as compared to 2002–2009) and a balancing decrease in the transport of the Deep Western Boundary Current (Koelling et al., 2020). The weakening of the Deep Western Boundary Current associated with the increased Gulf Stream instability and consequent eddy shedding, observed since 2008–2009, resembles the intrinsic variability previously predicted numerically (Spall, 1996). The high Gulf Stream stability in previous decades (combined with a strong Deep Western Boundary Current) was followed by a period of low Gulf Stream stability and weak Deep Western Boundary Current, which is associated with increased warm-core eddy activity north of the Gulf Stream and could, in turn, be associated with the recurrent diversion of the Labrador Current.

Even as the Lagrangian analysis presented here reveals how the variable Gulf Stream proximity to the Grand Banks influences the continuity of the Labrador Current, a broader question remains unanswered: What oceanographic or climatic changes cause these fluctuations in the Gulf Stream? A recent analysis of a high-resolution coupled climate model provides one possible hypothesis. Deep mixed layers and strengthened water mass formation in the western subpolar gyre are shown to thicken the deep Labrador Sea Water layer and lead to depressed sea surface height anomalies that move southward from the Labrador Sea to the Grand Banks (Yeager et al., 2021). It is plausible that thickened lower layer helps keep the valve open at the Tail of the Grand Banks, while its thinning might allow for the Gulf Stream to encroach toward the Grand Banks, although further study would be necessary to explore that hypothesis.

The timing of the declining Labrador Current connectivity is broadly consistent with the hypothesized connection between Labrador Sea Water (LSW) thickness and valving of the Tail of the Grand Banks: 1994 marked the end of a multi-year period of vigorous LSW formation resulting in the thickest LSW layer in 80 years of regular observations (Yashayaev & Loder, 2016). Between 1994 and 2015, LSW thickness generally declined, returning to strong formation in 2015/2016, right at the conclusion of the HYCOM simulation. Therefore, the open valve at the Tail of the Grand Banks corresponds with the period when the thick LSW was circulating through the Labrador Sea, and the open-valve occurs after 14 years of increasing stratification and thinning of the LSW. However, it is difficult to draw conclusions from the short period of overlapping observations and simulation years, and it must be noted that the winter of 2008 was actually a year of dense LSW formation, though a return to vigorous convection in that one winter was too brief to cause a wide-spread thickening of the LSW.

In Yeager et al. (2021), the sea surface height anomalies are also correlated with the strength of the AMOC. In our proposed two-layer conceptual framework, the blocking of the lower layer could also prevent the equatorward advection of the deep AMOC limb. Therefore, the fluctuating continuity of the Labrador Current at the Tail of the Grand Banks could help explain the association between the Northwest Atlantic Shelf warming and the AMOC slowing found in a high-resolution model (Caesar et al., 2018). These trends are expected to continue during this century under continuous greenhouse gas emissions (Saba et al., 2015).

The expected trends in Northwest Atlantic warming combined with the AMOC slowdown could pose serious environmental threats to the local environment and economy. Understanding the mechanisms responsible for rapid shelf warming like the one described here is vital to allow for anticipated responses to these threats. Marine heatwaves, for example, have become more common in recent years, after the shift in 2008, with massive events since 2012 (Mills et al., 2013; Pershing et al., 2018). These extreme events are expected to become more intense and frequent worldwide (Frölicher et al., 2018), although the prediction of both their intensity and frequency in the Atlantic under global warming are still highly uncertain (Plecha et al., 2021).

Establishing the connection between Northwest Atlantic warming and its atmospheric drivers (Chen et al., 2014), ocean advection (Gawarkiewicz et al., 2019), and, possibly, AMOC decline can help predict these long-term changes and extreme events. Extending this Lagrangian analysis to deeper layers within the Labrador Sea Water and the Overflow Waters could provide insight into this possible connection and help understand the degree to which the offshore diversion of the Labrador Current promotes increased importance of interior pathways for the cold branch of the AMOC (Koelling et al., 2020).

Data Availability Statement

The full-resolution HYCOM outputs are stored in the U.S. Army Engineer Research and Development Center (ERDC) archive server. The model results presented in this study are available in a data repository (Gonçalves Neto et al., 2022). The Matlab codes used in this study are available on GitHub (Gonçalves Neto, 2022).

Acknowledgments
The authors gratefully acknowledge funding from NOAA Climate Variability Program (Project #0008287) and valuable conversations with Tom Rossby and Kathy Donohue, which sharpened our synthesis.

References

Andres, M. (2016). On the recent destabilization of the Gulf Stream path downstream of Cape Hatteras. *Geophysical Research Letters*, *43*(18), 9836–9842. https://doi.org/10.1002/2016GL069966

Andres, M., Donohue, K. A., & Toole, J. M. (2020). The Gulf Stream's path and time-averaged velocity structure and transport at 68.5°W and 70.3°W. *Deep Sea Research Part I: Oceanographic Research Papers*, *156*, 103179. https://doi.org/10.1016/j.dsr.2019.103179

Biló, T. C., & Johns, W. E. (2019). Interior pathways of Labrador Sea Water in the North atlantic from the Argo perspective. *Geophysical Research Letters*, *46*(6), 3340–3348. https://doi.org/10.1029/2018GL081439

Bleck, R. (2002). An oceanic general circulation model framed in hybrid isopycnic-Cartesian coordinates. *Ocean Modelling*, *4*(1), 55–88. https://doi.org/10.1016/S1463-5003(01)00012-9

Bower, A. S., Lozier, S., & Gary, S. (2011). Export of Labrador Sea water from the subpolar North atlantic: A Lagrangian perspective. *Deep Sea Research Part II: Topical Studies in Oceanography*, *58*(17–18), 1798–1818. https://doi.org/10.1016/j.dsr2.2010.10.060

Bower, A. S., Lozier, M. S., Gary, S. F., & Böning, C. W. (2009). Interior pathways of the North Atlantic meridional overturning circulation. *Nature*, *459*(7244), 243–247. https://doi.org/10.1038/nature07979

Brickman, D., Hebert, D., & Wang, Z. (2018). Mechanism for the recent ocean warming events on the Scotian Shelf of eastern Canada. *Continental Shelf Research*, *156*, 11–22. https://doi.org/10.1016/j.csr.2018.01.001

Bulgin, C. E., Merchant, C. J., & Ferreira, D. (2020). Tendencies, variability and persistence of sea surface temperature anomalies. *Scientific Reports*, *10*(1), 7986. https://doi.org/10.1038/s41598-020-64785-9

Caesar, L., Rahmstorf, S., Robinson, A., Feulner, G., & Saba, V. (2018). Observed fingerprint of a weakening Atlantic Ocean overturning circulation. *Nature*, *556*(7700), 191–196. https://doi.org/10.1038/s41586-018-0006-5

Chassignet, E. P., & Marshall, D. P. (2008). Gulf Stream separation in numerical ocean models. In M. W. Hecht, & H. Hasumi (Eds.), *Geophysical Monograph series* (Vol. 177, pp. 39–61). American Geophysical Union. https://doi.org/10.1029/177GM05

Chassignet, E. P., Smith, L. T., Halliwell, G. R., & Bleck, R. (2003). North Atlantic simulations with the hybrid coordinate Ocean Model (HYCOM): Impact of the vertical coordinate choice, reference pressure, and thermobaricity. *Journal of Physical Oceanography*, *33*(12), 23–2526. https://doi.org/10.1175/1520-0485(2003)033⟨2504:NASWTH⟩2.0.CO;2

Chassignet, E. P., & Xu, X. (2017). Impact of horizontal resolution (1/12° to 1/50°) on Gulf stream separation, penetration, and variability. *Journal of Physical Oceanography*, *47*(8), 1999–2021. https://doi.org/10.1175/JPO-D-17-0031.1

Chen, K., Gawarkiewicz, G. G., Lentz, S. J., & Bane, J. M. (2014). Diagnosing the warming of the northeastern U.S. Coastal ocean in 2012: A linkage between the atmospheric jet stream variability and ocean response: Diagnosing the coastal warming in 2012. *Journal of Geophysical Research: Oceans*, *119*(1), 218–227. https://doi.org/10.1002/2013JC009393

Chi, L., Wolfe, C. L., & Hameed, S. (2018). Intercomparison of the Gulf stream in ocean reanalyses: 1993-2010. *Ocean Modelling*, *125*, 1–21. https://doi.org/10.1016/j.ocemod.2018.02.008

Claret, M., Galbraith, E. D., Palter, J. B., Bianchi, D., Fennel, K., Gilbert, D., & Dunne, J. P. (2018). Rapid coastal deoxygenation due to ocean circulation shift in the northwest Atlantic. *Nature Climate Change*, *8*(10), 868–872. https://doi.org/10.1038/s41558-018-0263-1

Delandmeter, P., & van Sebille, E. (2019). The parcels v2.0 Lagrangian framework: New field interpolation schemes. *Geoscientific Model Development*, *12*(8), 3571–3584. https://doi.org/10.5194/gmd-12-3571-2019

Dormand, J., & Prince, P. (1980). A family of embedded Runge-Kutta formulae. *Journal of Computational and Applied Mathematics*, *6*(1), 19–26. https://doi.org/10.1016/0771-050X(80)90013-3

Fischer, J., Schott, F. A., & Dengler, M. (2004). Boundary circulation at the exit of the Labrador Sea. *Journal of Physical Oceanography*, *34*(7), 1548–1570. https://doi.org/10.1175/1520-0485(2004)034⟨1548:BCATEO⟩2.0.CO;2

Fischer, J., Visbeck, M., Zantopp, R., & Nunes, N. (2010). Interannual to decadal variability of outflow from the Labrador Sea: Labrador sea outflow variability. *Geophysical Research Letters*, *37*(24), n/a–n/a. https://doi.org/10.1029/2010GL045321

Fratantoni, P. S., & McCartney, M. S. (2009). Freshwater export from the Labrador current to the North atlantic current at the Tail of the Grand Banks of Newfoundland. *Deep Sea Research Part I: Oceanographic Research Papers*, *57*(2), 258–283. https://doi.org/10.1016/j.dsr.2009.11.006

Fratantoni, P. S., & Pickart, R. S. (2007). The Western North Atlantic shelfbreak current system in summer. *Journal of Physical Oceanography*, *37*(10), 2509–2533. https://doi.org/10.1175/JPO3123.1

Frölicher, T. L., Fischer, E. M., & Gruber, N. (2018). Marine heatwaves under global warming. *Nature*, *560*(7718), 360–364. https://doi.org/10.1038/s41586-018-0383-9

Gary, S. F., Susan Lozier, M., Böning, C. W., & Biastoch, A. (2011). Deciphering the pathways for the deep limb of the meridional overturning circulation. *Deep Sea Research Part II: Topical Studies in Oceanography*, *58*(17–18), 1781–1797. https://doi.org/10.1016/j.dsr2.2010.10.059

Gawarkiewicz, G., Chen, K., Forsyth, J., Bahr, F., Mercer, A. M., Ellertson, A., et al. (2019). Characteristics of an advective marine heatwave in the middle atlantic Bight in early 2017. *Frontiers in Marine Science*, *6*, 712. https://doi.org/10.3389/fmars.2019.00712

Gonçalves Neto, A. (2022). Temporal variability of the Labrador Current pathways around the Tail of the Grand Banks at intermediate depths in a high-resolution ocean circulation model [Software]. Retrieved from https://github.com/afonsogneto/Matlab/blob/main/GoncalvesNeto_et_al_2022_JGRO.m

Gonçalves Neto, A., Palter, J. B., Xu, X., & Fratantoni, P. (2022). Temporal variability of the westward Labrador Current transport at the Tail of the Grand Banks [Dataset]. Zenodo. https://doi.org/10.5281/zenodo.6842581

Gonçalves Neto, A., Langan, J. A., & Palter, J. B. (2021). Changes in the Gulf stream preceded rapid warming of the Northwest Atlantic shelf. *Communications Earth & Environment*, *2*(1), 74. https://doi.org/10.1038/s43247-021-00143-5

Gonçalves Neto, A., Palter, J. B., Bower, A., Furey, H., & Xu, X. (2020). Labrador Sea water transport across the Charlie-Gibbs fracture Zone. *Journal of Geophysical Research: Oceans*, *125*(8). https://doi.org/10.1029/2020JC016068

Halliwell, G. R. (2004). Evaluation of vertical coordinate and vertical mixing algorithms in the HYbrid-Coordinate Ocean Model (HYCOM). *Ocean Modelling*, *7*(3–4), 285–322. https://doi.org/10.1016/j.ocemod.2003.10.002

Han, G., Lu, Z., Wang, Z., Helbig, J., Chen, N., & de Young, B. (2008). Seasonal variability of the Labrador current and shelf circulation off Newfoundland. *Journal of Geophysical Research*, *113*(C10), C10013. https://doi.org/10.1029/2007JC004376

Jones, B. T., Solow, A., & Ji, R. (2016). Resource Allocation for Lagrangian tracking. *Journal of Atmospheric and Oceanic Technology*, *33*(6), 1225–1235. https://doi.org/10.1175/JTECH-D-15-0115.1

Koelling, J., Send, U., & Lankhorst, M. (2020). Decadal strengthening of interior flow of North Atlantic deep water observed by GRACE satellites. *Journal of Geophysical Research: Oceans*, *125*(11). https://doi.org/10.1029/2020JC016217

Lange, M., & van Sebille, E. (2017). Parcels v0.9: Prototyping a Lagrangian ocean analysis framework for the petascale age. *Geoscientific Model Development*, *10*(11), 4175–4186. https://doi.org/10.5194/gmd-10-4175-2017

Lauzier, L. M. (1965). Long-term temperature variations in the Scotian Shelf area. *ICNAF Special Publication*, *6*, 807–816.

Lozier, M. S., Gary, S. F., & Bower, A. S. (2012). Simulated pathways of the overflow waters in the North Atlantic: Subpolar to subtropical export. *Deep Sea Research Part II: Topical Studies in Oceanography*, *85*, 147–153. https://doi.org/10.1016/j.dsr2.2012.07.037

Meyer-Gutbrod, E., Greene, C., Davies, K., & Johns, D. (2021). Ocean regime shift is driving collapse of the North atlantic right whale population. *Oceanography*, *34*(3), 22–31. https://doi.org/10.5670/oceanog.2021.308

Mills, K., Pershing, A., Brown, C., Chen, Y., Chiang, F.-S., Holland, D., et al. (2013). Fisheries management in a changing climate: Lessons from the 2012 ocean heat wave in the Northwest Atlantic. *Oceanography*, *26*(2). https://doi.org/10.5670/oceanog.2013.27

N. F. S. C. (2021). State of the ecosystem 2021: Mid-Atlantic Revised. https://doi.org/10.25923/JD1W-DC26

Pershing, A. J., Mills, K., Dayton, A., Franklin, B., & Kennedy, B. (2018). Evidence for Adaptation from the 2016 marine heatwave in the Northwest Atlantic ocean. *Oceanography*, *31*(2). https://doi.org/10.5670/oceanog.2018.213

Plecha, S. M., Soares, P. M. M., Silva-Fernandes, S. M., & Cabos, W. (2021). On the uncertainty of future projections of marine heatwave events in the North Atlantic Ocean. *Climate Dynamics*, *56*(7–8), 2027–2056. https://doi.org/10.1007/s00382-020-05529-3

Ramp, S. R., Schlitz, R. J., & Wright, W. R. (1985). The deep flow through the Northeast channel, Gulf of Maine. *Journal of Physical Oceanography*, *15*(12), 1790–1808. https://doi.org/10.1175/1520-0485(1985)015<1790:tdfttn>2.0.co;2

Rosmond, T., Teixeira, J., Peng, M., Hogan, T., & Pauley, R. (2002). Navy operational global atmospheric prediction system (NOGAPS): Forcing for ocean models. *Oceanography*, *15*(1), 99–108. https://doi.org/10.5670/oceanog.2002.40

Saba, V. S., Griffies, S. M., Anderson, W. G., Winton, M., Alexander, M. A., Delworth, T. L., et al. (2015). Enhanced warming of the Northwest Atlantic ocean under climate change. *Journal of Geophysical Research: Oceans*, *121*(1), 118–132. https://doi.org/10.1002/2015JC011346

Schott, F. A., Zantopp, R., Stramma, L., Dengler, M., Fischer, J. R., & Wibaux, M. (2004). Circulation and deep-water export at the Western Exit of the Subpolar North atlantic. *Journal of Physical Oceanography*, *34*(4), 27–843. https://doi.org/10.1175/1520-0485(2004)034⟨0817:CADEAT⟩2.0.CO;2

Silver, A., Gangopadhyay, A., Gawarkiewicz, G., Silva, E. N. S., & Clark, J. (2021). Interannual and seasonal asymmetries in Gulf stream ring formations from 1980 to 2019. *Scientific Reports*, *11*(1), 2207. https://doi.org/10.1038/s41598-021-81827-y

Solodoch, A., McWilliams, J. C., Stewart, A. L., Gula, J., & Renault, L. (2020). Why does the deep Western boundary current "leak" around Flemish Cap? *Journal of Physical Oceanography*, *50*(7), 1989–2016. https://doi.org/10.1175/JPO-D-19-0247.1

Spall, M. (1996). Dynamics of the Gulf stream/deep Western Boundary current Corssover. Part II: Low-frequency internal oscillations. *Journal of Physical Oceanography*, *26*(10), 2169–2182. https://doi.org/10.1175/1520-0485(1996)026<2169:dotgsw>2.0.co;2

Stommel, H., & Arons, A. (1959). On the abyssal circulation of the world ocean—I. Stationary planetary flow patterns on a sphere. *Deep Sea Research (1953)*, *6*(6), 140–154. https://doi.org/10.1016/0146-6313(59)90065-6

Uppala, S. M., Kållberg, P. W., Simmons, A. J., Andrae, U., Bechtold, V. D. C., Fiorino, M., et al. (2005). The ERA-40 re-analysis. *Quarterly Journal of the Royal Meteorological Society*, *131*(612), 2961–3012. https://doi.org/10.1256/qj.04.176

van Sebille, E., Griffies, S. M., Abernathey, R., Adams, T. P., Berloff, P., Biastoch, A., et al. (2018). Lagrangian ocean analysis: Fundamentals and practices. *Ocean Modelling*, *121*, 49–75. https://doi.org/10.1016/j.ocemod.2017.11.008

Wang, Z., Yashayaev, I., & Greenan, B. (2015). Seasonality of the inshore Labrador current over the Newfoundland shelf. *Continental Shelf Research*, *100*, 1–10. https://doi.org/10.1016/j.csr.2015.03.010

Xu, X., Bower, A., Furey, H., & Chassignet, E. P. (2018). Variability of the Iceland-Scotland overflow water transport through the Charlie-Gibbs fracture zone: Results from an eddying simulation and observations. *Journal of Geophysical Research: Oceans*, *123*(8), 5808–5823. https://doi.org/10.1029/2018JC013895

Xu, X., Hurlburt, H. E., Schmitz, W. J., Zantopp, R., Fischer, J., & Hogan, P. J. (2013). On the currents and transports connected with the atlantic meridional overturning circulation in the subpolar North Atlantic. *Journal of Geophysical Research: Oceans*, *118*(1), 502–516. https://doi.org/10.1002/jgrc.20065

Xu, X., Rhines, P. B., Chassignet, E. P., & Schmitz, W. J. (2015). Spreading of Denmark strait overflow water in the Western Subpolar North atlantic: Insights from eddy-resolving simulations with a passive tracer. *Journal of Physical Oceanography*, *45*(12), 2913–2932. https://doi.org/10.1175/JPO-D-14-0179.1

Yashayaev, I., & Loder, J. W. (2016). Recurrent replenishment of Labrador Sea Water and associated decadal-scale variability: 2015 convection in Labrador Sea. *Journal of Geophysical Research: Oceans*, *121*(11), 8095–8114. https://doi.org/10.1002/2016JC012046

Yeager, S. G., Castruccio, F., Chang, P., Danabasoglu, G., Maroon, E., Small, J., et al. (2021). An outsized role for the Labrador Sea in the multidecadal variability of the Atlantic overturning circulation. *Science Advances*, *7*(41), 1–14. https://doi.org/10.1126/sciadv.abh3592